



## Absorbed dose evaluation of a blood irradiator with alanine, TLD-100 and ionization chamber

S. Grasso<sup>a</sup>, A. Varallo<sup>a,b</sup>, R. Ricciardi<sup>a,b</sup>, M.E. Italiano<sup>a</sup>, C. Oliviero<sup>c</sup>, V. D'Avino<sup>d</sup>, C. Feoli<sup>e</sup>, F. Ambrosino<sup>d</sup>, M. Pugliese<sup>d,\*</sup>, S. Clemente<sup>c</sup>

<sup>a</sup> Post Graduate School in Medical Physics, University of Naples Federico II, 80131, Naples, Italy

<sup>b</sup> National Institute of Nuclear Physics, 80126, Naples, Italy

<sup>c</sup> Unit of Medical Physics and Radioprotection, A.O.U Policlinico Federico II, 80131, Naples, Italy

<sup>d</sup> Department of Physics "E. Pancini", University of Naples Federico II, 80126, Naples, Italy

<sup>e</sup> Department of Advanced Biomedical Sciences, University of Naples Federico II, 80131, Naples, Italy

### ARTICLE INFO

#### Keywords:

Blood irradiation X-Ray irradiator  
Raycell MK2  
Dose mapping  
Alanine  
Ion chamber  
TLD dosimetry

### ABSTRACT

Irradiation of blood bags using X-ray irradiators and dosimetry services are required to ensure uniform dose levels in the range 25–50 Gy to prevent Transfusion Associated Graft versus Host Disease (TA-GvHD). An absorbed dose characterization of a Raycell MK2 X-Irradiator was performed using three different dosimetric systems. Results showed a dosimetric accuracy of the ionization chamber together with the Alanine dosimeter. TLDs measurements exhibited a small overestimation by 4% of the absorbed dose. The Dose Uniformity Ratio (DUR), between maximum and minimum dose levels in the canister, was in good agreement with the manufacturer specifications ( $\leq 1.5$ ).

### 1. Introduction

Blood irradiation is a standard procedure adopted by clinicians to prevent Transfusion Associated Graft versus Host Disease (TA-GvHD) that can affect immunocompromised patients. The target of the irradiation is the DNA of the T-lymphocytes, that is intentionally damaged to inactivate their capability to multiply and then increase the risk of TA-GvHD in vulnerable subjects (Treleaven, et al., 2010). Irradiation techniques for healthcare and industrial applications (Bartolotta et al., 1989; Nasreddine et al., 2021; Sharpe et al., 1996), were based for long time on gamma radiation from radioactive sources like Cesium ( $^{137}\text{Cs}$ ) and Cobalt  $^{60}\text{Co}$  (Bakri et al., 2021; Tadokoro et al., 2010), but in recent years, there was an increasing interest in the use of kilovoltage X-ray photons for blood irradiation. It was demonstrated (Bashir et al., 2011) that X-irradiation produces acceptable effects on the quality of the red cells (i.e. good levels of hemolysis and potassium leakage) without reducing the effectiveness of inactivation of the T-lymphocytes (Cleland and Stichelbaut, 2013; Dodd and Vetter, 2009). Therefore the technique was recommended by the US National Academy of Sciences (US National Academy of Science, 2008). In line with this, our University Hospital was equipped with a Raycell MK2 X-ray irradiator (Best Theratronics

Ltd, 2011) for blood irradiation at dose levels in the range 25–50 Gy with a lower limit of 15 Gy in any peripheral point, according to the guidelines of the American Authorities (Association for the Advancement of Blood & Biotherapies), (FDA-Food & Drug Administration) and as referred in the literature (Jacobs, 1998; Soares et al., 2009). Recently, a Raycell MK2 irradiator was characterized by Simuta et al. (2021) at a dose of 100 Gy for the sterile insect technique (SIT), measuring the dose distribution inside the canister with different dosimeters (e.g. radiochromic films). It is important that the real absorbed dose corresponds to the predicted value, as dose levels below 15 Gy would cause residual TA-GvHD risk, while doses beyond 50 Gy could damage the transfusion blood with potential risk of erythrocytes corruption (Jacobs, 1998) or even induced radioactivity (Frentzel and Badakhshi, 2016). Reliable dosimetry methods for accurate dose determination is recommended. Several techniques were validated and adopted as dosimetry systems. The alanine/EPR (electron paramagnetic resonance) dosimeters were widely adopted as a reference and transfer systems for high doses in industrial applications due to their suitable properties such as near water/tissue equivalence, small energy dependence and non-destructive, even if not immediate, read out (Sharpe et al., 1996). Application to X-ray synchrotron at very high dose rates ( $10^2$ – $10^4$  Gy/s)

\* Corresponding author.

E-mail address: [mpuglies@na.infn.it](mailto:mpuglies@na.infn.it) (M. Pugliese).

<https://doi.org/10.1016/j.apradiso.2023.110981>

Received 9 March 2023; Received in revised form 20 July 2023; Accepted 11 August 2023

Available online 12 August 2023

0969-8043/© 2023 The Authors. Published by Elsevier Ltd. This is an open access article under the CC BY license (<http://creativecommons.org/licenses/by/4.0/>).

was proposed by [Butler et al. \(2016\)](#) and by [Soliman et al. \(2020\)](#) for dose accuracy evaluation in radiation therapy, basic for the patients treatments and operators radiation protection. For low and medium energy range X-rays, it was reported ([Anton and Büermann, 2015](#); [Butler et al., 2016](#); [Waldeland et al., 2010](#)) that alanine/EPR response is energy dependent and in particular the relative response to kilovoltage X-ray irradiations with respect to  $^{60}\text{Co}$  beams can vary from 0,68 to 0,90 at 50 kV and 200 kV respectively. Thus, correction factors to the direct alanine measurements are to be applied in order to avoid dose underestimations ([Waldeland and Malinen, 2011](#)). Reference dosimetry based on ionization chambers calibrated to air kerma is commonly adopted for low and medium energy X-ray beams (40 kV–300 kV) ([Ma, et al., 2001](#)) in diagnostic radiology and also for radiotherapy and radiobiology. It allows reliable dose and dose rate measurements in real time read out. Furthermore, new ionization chamber dosimetry based on  $^{60}\text{Co}$  absorbed dose to water calibration has been proposed, where suitable coefficients can be used for the correct dose assessment ([Araki et al., 2018](#); [Tachibana et al., 2022](#)). Thermoluminescent Dosimeters (TLDs) are widely used in routine dosimetry for low and intermediate dose measurements (1–100 mGy) in the field of the radiation protection for the occupational exposures and the environmental monitoring ([D'Avino et al., 2022](#); [Del Sol Fernández et al., 2016](#)). Their use, particularly the standard model LiF:Mg,Ti (TLD-100), has been a standard since the 1960's and is commonly adopted in the medical diagnostic radiology and radiation therapy ([Hsi et al., 2013](#); [Rudén, 1976](#)). TLD-100 has several advantages, such as small size for measurements inside phantoms, near tissue equivalence for detecting tissue and organ dose ([Nikolovski et al., 2010](#)), sensitivity ([Liuzzi et al., 2015, 2020](#)), and a large dose range with precision better than 3% for doses in the range from 1 mGy to 10 Gy ([Horowitz, 1984](#)). At doses higher than 10 Gy, TLD-100 exhibits a supralinear dose response ([Knoll, 1999](#); [Reuven and Pagonis, 2019](#)). Radiochromic film (RCFs) dosimetry is another dosimetric technique, widely employed for its reliability, accuracy, ease of use and cost. RCFs are dosimeters based on the property of modifying the structural characteristics of their crystalline sensitive element when exposed to ionizing radiations. The interaction of radiation with the film produces a polymerization process in the monomers of the sensitive element. This microscopic phenomenon is reflected in a color change of the film at macroscopic level that can be related to the radiation dose ([Casolaro et al., 2019](#)). Different types of radiochromic films were available, each sensitive to a particular dose range ([Ashland Advanced Materials Company, 2023](#)). A dosimetric characterization of a Raycell MK2 X-Irradiator was performed using three of these systems: a specially made alanine phantom provided by the Supplier Best Theratronics Ltd, (Ottawa, Canada), an ion chamber and TLD-100 dosimeters. The dose uniformity in the canister, the volume containing the blood bags, was investigated. A set of dose measurements in free air was also performed using the ion chamber.

## 2. Materials and methods

### 2.1. The blood irradiator

Our Department of Hematology was equipped with a Raycell MK2, an X-ray irradiator manufactured by the Company Best Theratronics Ltd, for the primary purpose of sterilizing blood bags to inactivate T-lymphocytes and prevent TA-GvHD in immunocompromised patients ([Best Theratronics Ltd, 2011](#)). The irradiator looks like a metal case  $1525 \times 1450 \times 1000 \text{ mm}^3$  where two opposing X-ray tubes, managed by an auxiliary equipment, are installed for the irradiation of a canister containing the blood bags. The plastic canister shielded with graphite has a cylindrical form with 167 mm diameter and 97 mm height, corresponding to a total capacity of 2.0 L, which allows to house and irradiate at the same time up to 4 bags (300 ml each) or 2 bags (600 ml each) per cycle. The sample container is positioned centrally between the two X-ray tubes (see [Fig. 1](#)), to ensure that a uniform dose is delivered to the

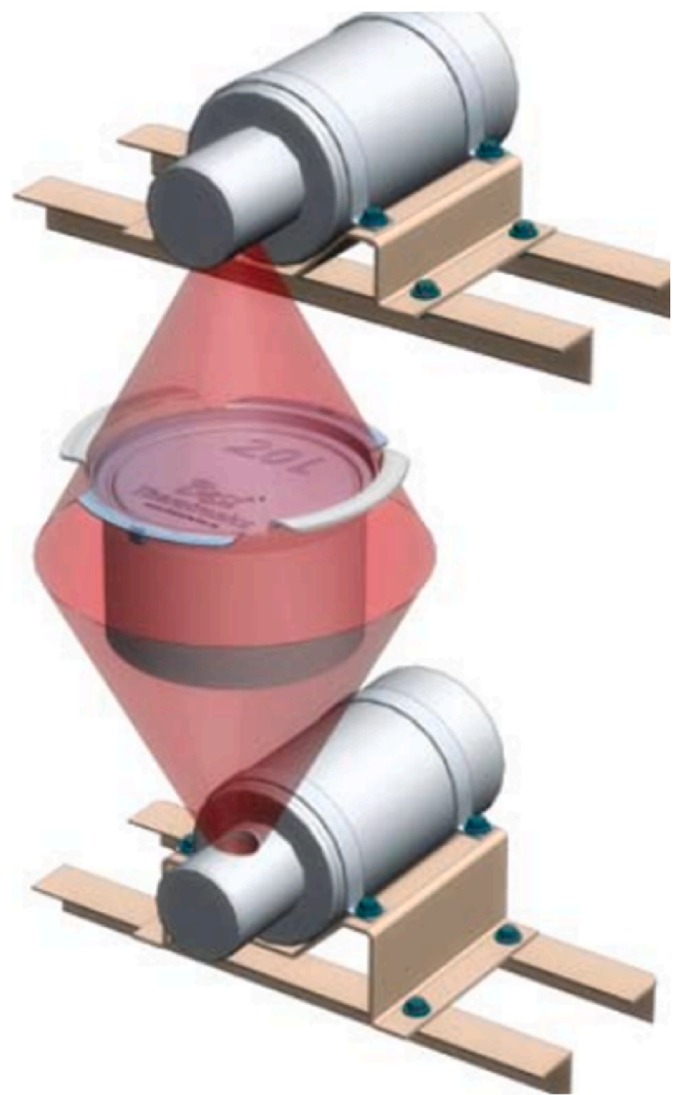


**Fig. 1.** Assembly of the sample container of the blood bags and the two opposing X-ray tubes in the Raycell MK2 irradiator.

bags.

The X-beam quality, with average energy in the range of 60–80 keV, is characterized by a tube voltage of 160 kVp,  $\text{HVL} = 7,4 \text{ mm Al}$  and by a current of 37,5 mA, while the inherent filtration is made of 4,3 mm Be plus 0,4 mm Cu. The central dose rate was set in our Hematology Department, to a constant value of 12,75 Gy/min and the dose delivery managed by changing the irradiation time. The set time for one cycle, to ensure the nominal irradiated dose of 37 Gy in the center of the sample container, was 2,9 min.

### 2.2. Dose in the canister and dosimetry systems

For the study, a polystyrene phantom containing alanine pellets, exactly matching with the 2 L (L) volume of the canister, was used. Then, for additional dose measurements, three horizontal layers at the top, middle and bottom of the canister, were identified. For each layer, five points of measurements were investigated: four in the cardinal edge positions (to a quarter of an hour) and one point in the center of the layers ([Fig. 2](#)).

#### 2.2.1. Alanine dosimeter

The cylindrical polystyrene phantom (ID T151027e) provided by Best Theratronics Ltd., perfectly matching with the 2 L canister, consists

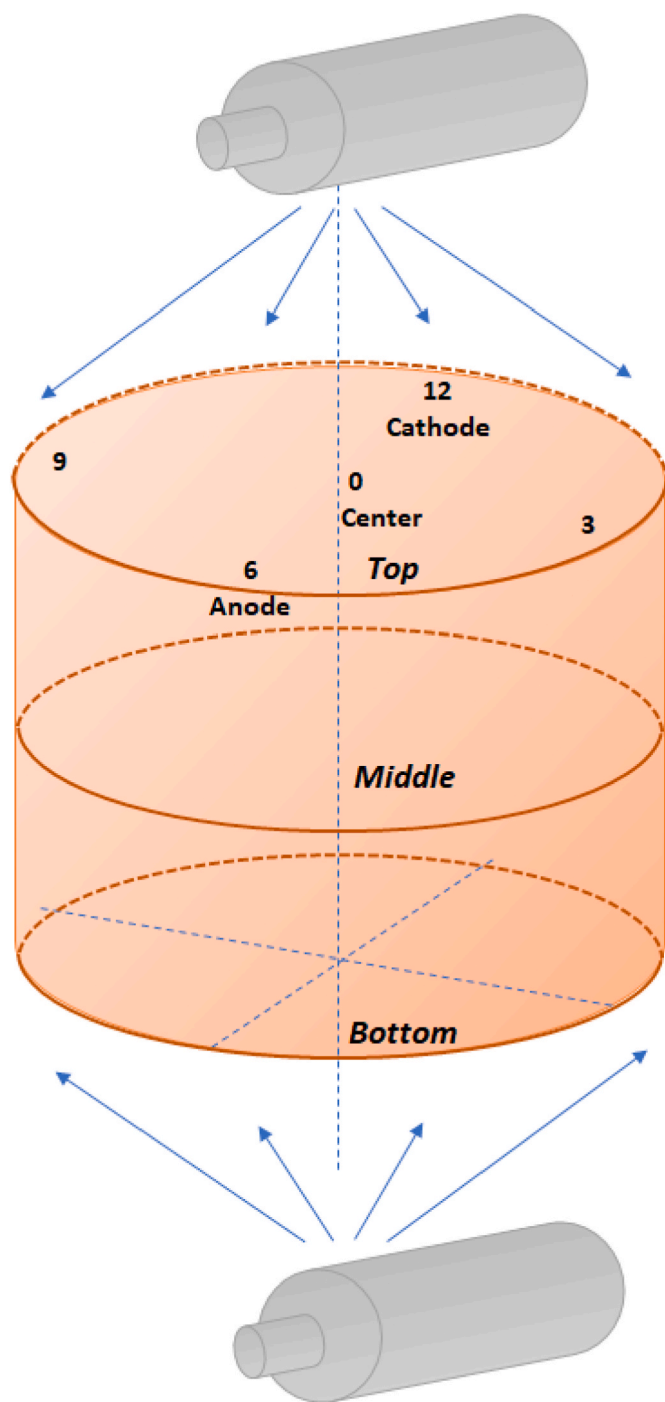


**Fig. 2.** The red volume represents the canister volume. The layers top, middle and bottom and the above numbers, the identified dose measurement points. Drawing is not to scale.

of 45 alanine dosimeters (pellets of 5 mm diameter and 1,5 mm height) embedded in the bulk of the phantom spread over the bottom, middle and the top layer (Fig. 3).

The polystyrene phantom placed into the canister, was irradiated at a nominal dose of 37 Gy, at a temperature of 25 °C (monitored with a thermometer HD 2307.0 DeltaOhm), and the alanine pellets processed by Best Theratronics, one week later using the EPR technique to get the dose information. The irradiated pellets were readout under controlled storage conditions (temperature, humidity) using an EPR spectrometer operated in the X-band. Parameters as electromagnetic field, microwave bridge and signal channels were optimized as crucial parameters to get

acceptable precision and reasonable readout time. The Alanine pellets were calibrated to the output of an ionization chamber, and the chamber was calibrated in medium-energy X-ray beam at an accredited lab traceable to a primary standard. AAPM TG-61 was used to convert the chamber's calibration in medium-energy X-ray beam to calibration in our Raycell beam.

### 2.2.2. Ionization chamber in PMMA phantom and in air

A Farmer type ionization chamber model 10x6-0,6 (Radcal Corporation, Monrovia, CA, USA) connected with an digitizer and an electrometer AccuDose Model ADDM, auto temperature and pressure compensated, was used for the real-time measurements. Both the ion chamber and the electrometer had certification in Co60-H1 gamma rays radiation with SDD (Source to Device Distance) equal to 800 mm and Dose Rate of 21,283 mGy/min. The calibration was performed by the Radcal Calibration Laboratory compatible to ISO 17025. In the technical data sheet provided by the manufacturer the correction factor for medium energy X-rays was in the range 0,97 to 1,01, and this was considered in the measurements performed in the present work. The ion chamber was embedded into a polymethyl methacrylate (PMMA) phantom, homemade as two rotating cylindrical sections suitable to place the chamber with the sensitive volume at the central and the cardinal edge positions of the three layers. A total amount of fifteen different positions, were investigated at a nominal dose of 37 Gy. Dose measurements were also performed in free air at the same fifteen positions of the canister at a nominal dose of 37 Gy.

### 2.2.3. Thermoluminescent dosimeters (TLDs)

LiF:Mg,Ti TLD dosimeters referred to as TLD-100, manufactured with a chip ( $3.2 \times 3.2 \times 0.9 \text{ mm}^3$ ) geometry by the Harshaw Chemical Company in Cleveland, OH (USA) were used for the study. LiF:Mg,Ti TLDs were housed, on an acrylonitrile-styrene-acrylate (ASA) support purpose built with a 3D printer (Fused Deposition Modelling 3D printing additive manufacturing) (Fig. 4), into the chamber inserts of the PMMA phantom, to occupy the same positions of the sensitive volume of the ion chamber and alanine pellets in the top and the middle layers (Fig. 4). LiF:Mg,Ti TLD dose in the bottom layer was not investigated because of the specific geometrical incompatibility of the ASA support in the PMMA phantom.

A total amount of ten different positions were investigated, using forty-four LiF:Mg,Ti TLD dosimeters (a matrix of four LiF:Mg,Ti TLDs at the cardinal edge positions and of six at the center of both layers), uniquely labelled with alphanumeric code, irradiated at the same nominal dose of 37 Gy. The average value of the LiF:Mg,Ti TLDs response was used as the best estimation of the dose punctually measured. The remaining fifteen LiF:Mg,Ti TLDs were used to determine the calibration curve. In Table 1 the correspondence of the dose measurement points using the three different methods was summarized.

Firstly, the daily output at the nominal irradiation time, in the middle layer and central position of the PMMA phantom, was measured using the ionization chamber. Prior to use all TLDs were first characterized by determining the relative intrinsic sensitivity factor ( $S_i$ ) that expresses the response variation of each individual dosimeter around the mean. Any TLD exhibiting a  $S_i$  greater than 10% was rejected, while the  $S_i$  of each selected TLD was used as a correction factor when we exposed it for dosimetric use. Then, arranging the LiF dosimeters in the ASA support at the same position, five dose values covering the range of interest between 25 and 40 Gy were set to determine the TLDs calibration curve. For each dose point, three TLDs provided the average readout ( $\mu\text{C}$ ), after the heating procedure made at the Radioactivity Laboratory of the "Ettore Pancini" Physics Department of the University of Naples Federico II. The reader system consisted of two main parts: the TL Reader Unit (Harshaw 3500) and the PC Unit equipped with the Thermo Scientific WinREMS readout Software (Waltham, MA, USA) (Model 3500 Manual TLD Reader, 1993). The TLDs readout was performed one day after the irradiation so that the fading effects were negligible. Prior

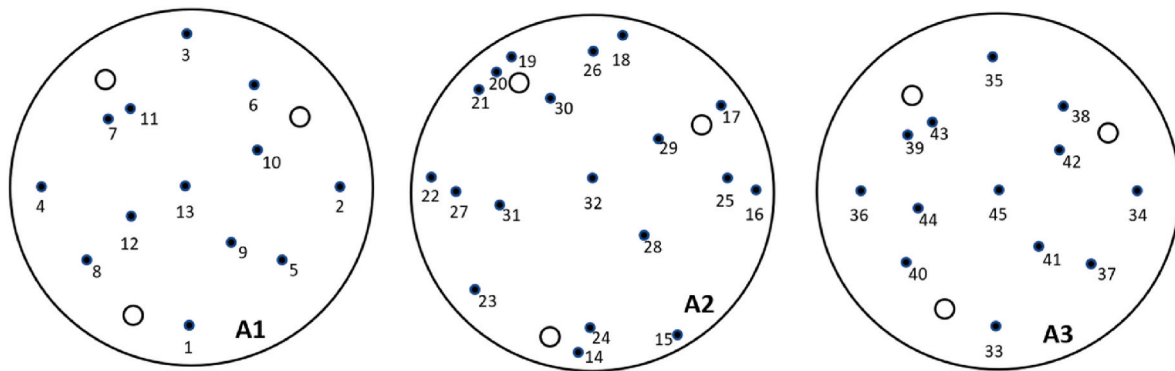


Fig. 3. Distribution of the 45 Alanine dosimeters over the three horizontal layers of the polystyrene phantom: A1 bottom, A2 middle, A3 top.



Fig. 4. ASA support A) for TLDs housing; B) inserted in the PMMA phantom.

Table 1

Corresponding measuring points in the Alanine and PMMA phantoms inside the canister.

Layer	Dosimeter position in the polystyrene/alanine phantom	Ion Chamber and LiF:Mg,Ti TLD position in PMMA phantom
Bottom	1	6 Anode
	2	3
	3	12 Cathode
	4	9
Middle	13	0 Central
	24	6 Anode
	25	3
	26	12 Cathode
	27	9
Top	32	0 Central
	33	6 Anode
	34	3
	35	12 Cathode
	36	9
	45	0 Central

to each use, the dosimeters were heated using an Isotemp programmable muffle furnace (Thermo Fisher Scientific, Waltham, MA, USA) following the standard procedure of LiF:Mg, Ti material consisting in a two-temperature process: 1 h at 400 °C followed by cooldown to 100 °C for 2 h. After irradiation, the TLDs were analyzed through the reading system consisting of two components: the Harshaw 3500 manual TL reader with planchet heating system and WinREMS readout software (Thermo Scientific, Waltham, MA, USA), allowing to set the acquisition setup parameters and to monitor the TLD reading process. TL measurements net from the gamma background were obtained by subtracting the reading of a non-irradiated TLDs group from the TL response of the irradiated ones.

### 3. Results

The average absorbed dose for the Alanine pellets, with an overall uncertainty of ±9% at the 95% confidence level, was  $37,28 \pm 0,87$  Gy, resulting in a good agreement with the nominal dose value of 37 Gy. The minimum dose of  $32,36 \pm 2,91$  Gy was recorded at the anode side in the middle layer (point six), while the maximum of  $39,92 \pm 3,59$  Gy at the point 3 in the top layer. The Dose Uniformity Ratio (DUR), calculated as the ratio between maximum and minimum dose level in the canister, was equal to 1.23. The dose values by the ionization chamber in the PMMA phantom were collected in real time during the experimental activities with an overall uncertainty of ±5%, as reported in the calibration certificate. The average dose was  $37,00 \pm 0,48$  Gy, perfectly matching the nominal value. The minimum dose of  $33,96 \pm 2,91$  Gy was recorded as before at the anode side in the middle layer while the maximum of  $39,39 \pm 3,59$  Gy at coordinate 3 of the top layer. The DUR was equal to 1.16. In free air the average dose measured by the ionization chamber was  $38,13 \pm 0,49$  Gy. The minimum dose of  $33,26 \pm 1,66$  Gy was recorded at the central axis (coordinate 0) in the middle layer while the maximum of  $40,10 \pm 2,01$  Gy at coordinate 3 of the top layer. The DUR was equal to 1.21. The LiF:Mg,Ti TLD-100 calibration curve, in the range 25–40 Gy was approximated to a linear response with a regression of  $R^2 = 0,99$  (see Fig. 5).

The regression analysis was performed to verify that the linear relationship between TL response and absorbed dose could be considered a good approximation. The goodness of fit was assessed by the  $R^2$  coefficient. The calibration factor was applied to the reading values of each LiF:Mg,Ti TLDs exposed in the PMMA phantom. The corresponding error was calculated by taking into account the uncertainties of the calibration factor and response provided by the TL reader (5% of the reading). The average dose was  $38,54 \pm 0,18$  Gy, overestimating the nominal dose value by 4%. The minimum dose of  $35,07 \pm 0,51$  Gy was

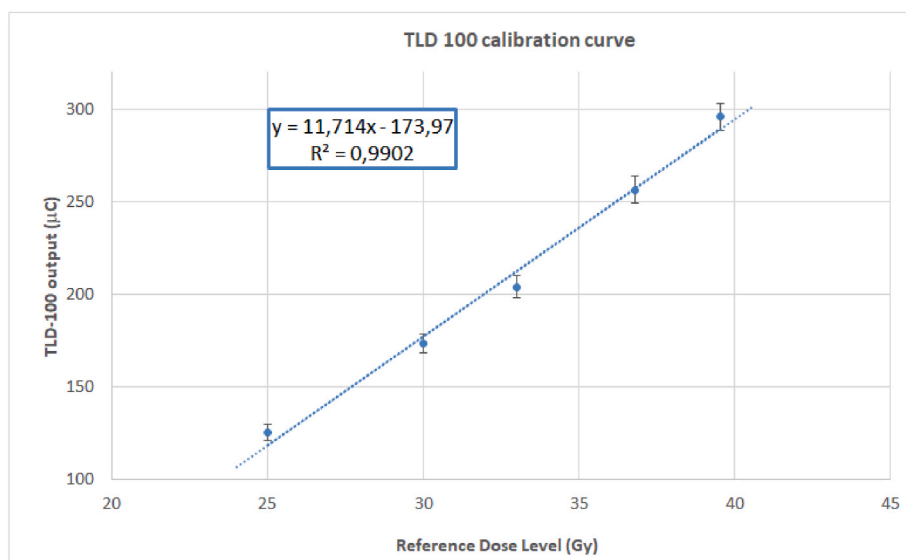


Fig. 5. Calibration curve approximated by a linear regression of the Thermoluminescent Dosimeters (TLDs) exposed to X-ray beams of the Raycell blood irradiator in the dose range 25–40 Gy. The  $R^2$  and linear equation are reported inside the graph. TL output, expressed in  $\mu\text{C}$ , is the average of three single LiF:Mg,Ti TLDs put in an array on the ASA support at the center of the canister; thus, the overall uncertainty comes from the propagation formula of each single TL error equal to  $\pm 5\%$ .

recorded at the anode side in the middle layer and the maximum of  $42,34 \pm 0,69$  Gy at coordinate 3 of the top layer. The DUR resulted equal to 1.21 (calculated on two of the three layers). Detailed data are reported in Table 2.

The uncertainties of the calculated results (i.e. the average values) were derived by the propagation of errors formula, as shown in Table 3.

Figs. 6 and 7 respectively show the average doses along the vertical axis and over the three horizontal layers of the canister, obtained using the different dosimetric approaches.

#### 4. Discussion

From the collected results, we found that measurements of dose levels in the sample container, at clinical operating conditions (160 kVp, 2,9 min, tissue equivalent material), confirmed the nominal doses declared by the manufacturer. The Alanine dosimeter and ionization chamber proved to be reliable dosimetry systems for the quality check of the blood irradiator: in fact, the average dose in the irradiated volume resulted in agreement with the nominal value of 37 Gy. Furthermore, the dose uniformity ratio was well below the maximum level ( $\text{DUR} = 1.5$ ) declared by the manufacturer, as also reported by Simuta et al. (2021),

who analyzed the same irradiator model (Simuta et al., 2021), the DUR estimated resulted widely below the specifications. Only in the LiF:Mg,Ti TLDs measurements, a slight overestimation of the average dose was observed, which could be due to the supralinearity effects. Nevertheless, the DUR was below 1.5, which allows to consider the Li:F:Mg,Ti detectors howsoever suitable for periodic quality assurance of the dose uniformity into the canister of the blood-irradiator. It's fair to note that supralinear response of thermoluminescent dosimeters above 10 Gy is reported by several literature studies. However this non-linear behavior of TL response don't affect our dose measurements since we restricted the calibration curve in the range 25–40 Gy where the linear trend results in a good approximation as showed in Fig. 5. It's should be mentioned that TLD light output was affected by the dependence from photon energy as assessed by Nunn et al. (2008). However were we calibrated the TLDs in the dose range of interest with the same X ray spectrum shape of blood irradiator used for dose evaluation with different dosimetric systems. For all three dosimetric systems, the maximum point dose measured always corresponded to the coordinate 3 on the top layer, which is in contrast with the symmetry of the tubes set-up. This could be due to a minor X ray tubes misalignment. On the other hand, the minimum level of dose was always measured at the coordinate 6 corresponding to the anode side in the middle layer, due to the combination of the Anode Heel Effect and the attenuation of the radiation into the phantom. The Anode Heel Effect can be quantified in Fig. 6, where dose reduction (of about 10%) can be observed along the peripheral vertical axis of the cylinder at the anode side. Similarly, Fig. 7 shows that the lowest average dose was recorded over the Middle plane, where the bulk of the phantom produces attenuation of the incident X-ray radiation intensity according to the Lambert Beer law for a polychromatic spectrum. The dose distribution inside the Raycell canister exhibits an hourglass dose profile due to the specific geometry of the two opposing X-ray tubes and attenuation described above.

#### 5. Conclusion

We performed a thorough characterization of the Raycell MK2 blood irradiation available in our Department of Hematology of the AOU Federico II of Naples (Italy) by measuring the absolute dose at standard operative conditions using an Alanine dosimeter phantom provided by the irradiator manufacturer and with two alternative systems, an ionization chamber and LiF:Mg,Ti TLDs dosimeters. Dose measured with

Table 2

Dose measurements in the Racycell canister at the 15 investigated coordinates. Data from alanine dosimetry are expressed in Gy with 9% uncertainty. Data from ionization chamber are expressed in Gy with 5% uncertainty. Finally, LiF:Mg,Ti TLDs data are expressed in Gy with 5% uncertainty and are referred to the 10 reference coordinates over the top and middle layer of the canister.

	Layer Position	0	12	3	6	9
		Central	Cathode		Anode	
Alanine	Top	38,74	39,67	39,92	38,15	39,78
	Middle	35,37	32,90	34,31	32,36	34,28
	Bottom	38,07	39,22	39,70	37,17	39,51
Ionization chamber in PMMA phantom	Top	37,35	37,69	39,39	35,04	38,07
	Middle	36,65	34,56	34,93	33,96	35,11
	Bottom	39,35	39,22	38,65	37,37	37,59
Ionization chamber in air	Top	34,53	39,78	40,10	37,06	39,98
	Middle	33,26	39,57	39,60	37,67	39,58
	Bottom	34,65	39,42	38,89	37,76	40,09
TLDs dose measurements	Top	36,33	41,34	42,34	41,59	42,21
	Middle	38,74	35,36	35,92	35,07	36,50

**Table 3**

Detail of the uncertainty of the measurements for the three dosimetry systems Alanine, Ion chamber and TLD.

Dosimetry	Uncertainty for a direct dose measurement $d_i$	Uncertainty for a calculated value $f = f(x_i)$ derived by $n$ direct measurements $x_i$ each with uncertainty $\Delta x_i$ (General formula of propagation of errors)	Uncertainty for average doses $\bar{D} = \frac{1}{n} \sum_{i=1}^n d_i$ derived by $n$ direct dose measurements $d_i$ each with uncertainty $\Delta d_i$
Alanine	9%	$\Delta f = \sqrt{\sum_{i=1}^n \left( \frac{\partial f}{\partial x_i} \Delta x_i \right)^2}$	$\Delta \bar{D} = \frac{1}{n} \sqrt{\sum_{i=1}^n (\Delta d_i)^2}$
Ion chamber	5%		
TLD	5%		

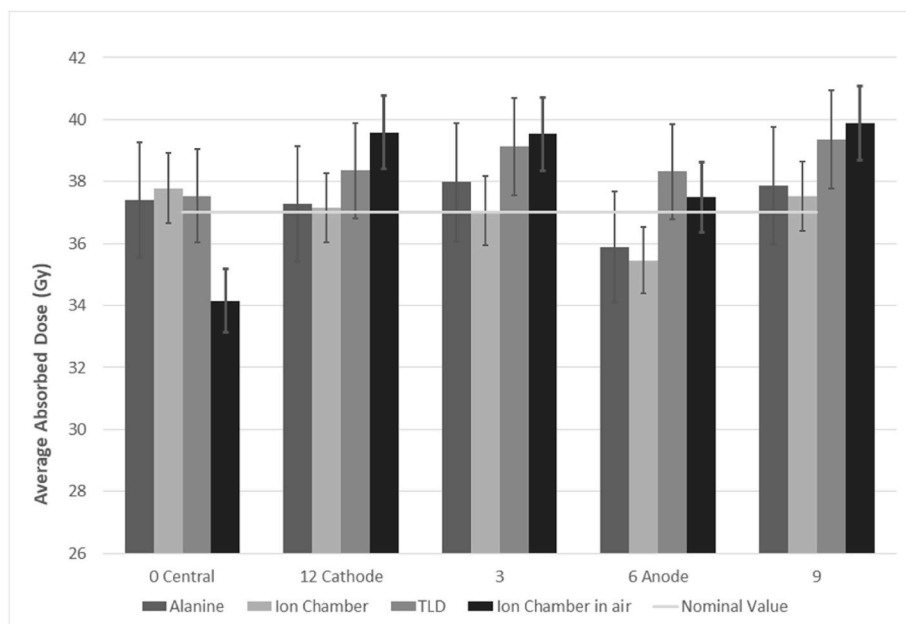


**Fig. 6.** Average absorbed dose along the vertical axes of the canister volume using the three dosimetric systems.

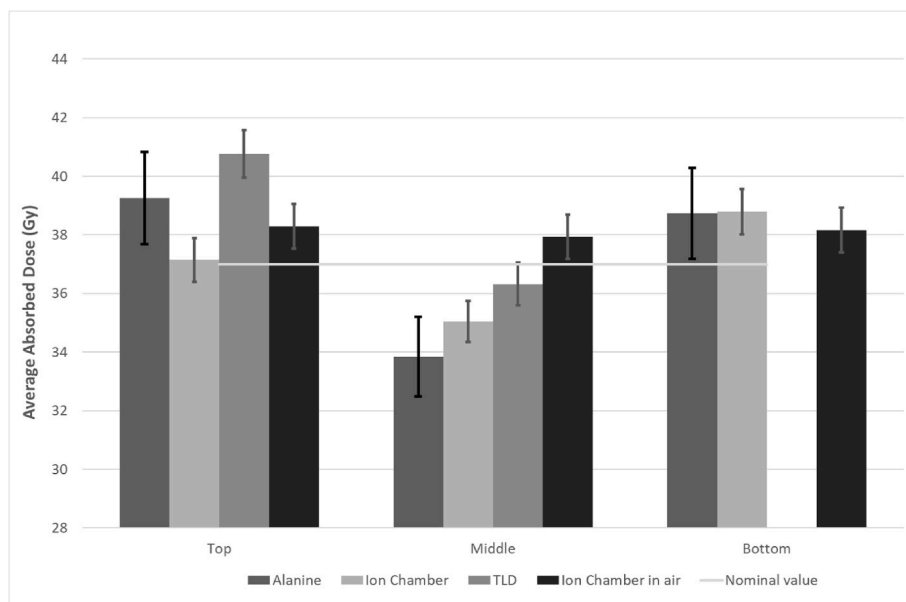


**Fig. 7.** Average absorbed dose over the three-horizontal top, middle and bottom layers of the canister volume. The Bottom layer with the LiF:Mg,Ti TLDs was not investigated.

Alanine and ionization chamber and the calculated DUR fully comply with the expectations, while LiF:Mg,Ti TLDs dose measurements are slightly overestimated. The Raycell Irradiator passed the quality tests

and is reliable for clinical application. The ionization chamber system is an equally reliable dosimetry system that can be used for periodic quality assurance tests in alternative to the Alanine pellets. For the LiF:

Mg,Ti TLDs dosimetry more investigations are necessary, to improve the reliability of the dose measurements, also in view of the several factors that can affect the final output such as the reading systems, the perpendicularity of the incident photons on the sensitive area and the calibration curve. Nevertheless, LiF:Mg,Ti TLDs can be just now used to test the relative dose uniformity. In the future steps, we are planning to simulate the irradiator with the Monte Carlo, to better characterize its technical aspects.

### CRedit authorship contribution statement

**S. Grasso:** Visualization, Validation, Resources, Project administration, Investigation, Funding acquisition, Conceptualization, Writing – original draft, Writing – review & editing. **A. Varallo:** Visualization, Validation, Resources, Methodology, Investigation, Funding acquisition, Data curation, Conceptualization, Writing – original draft, Writing – review & editing. **R. Ricciardi:** Visualization, Software, Investigation, Formal analysis, Data curation, Writing – review & editing. **M.E. Italiano:** Visualization, Software, Investigation, Data curation, Writing – review & editing. **C. Oliviero:** Visualization, Validation, Investigation, Data curation, Writing – review & editing. **V. D'Avino:** Visualization, Validation, Software, Methodology, Formal analysis, Data curation, Writing – review & editing. **C. Feoli:** Visualization, Validation, Investigation, Data curation, Writing – review & editing. **F. Ambrosino:** Visualization, Validation, Investigation, Data curation, Writing – review & editing. **M. Pugliese:** Visualization, Validation, Supervision, Resources, Project administration, Methodology, Investigation, Funding acquisition, Conceptualization, Writing – original draft, Writing – review & editing. **S. Clemente:** Visualization, Validation, Supervision, Resources, Project administration, Methodology, Investigation, Funding acquisition, Data curation, Conceptualization, Writing – original draft, Writing – review & editing.

### Declaration of competing interest

The authors declare that they have no known competing financial interests or personal relationships that could have appeared to influence the work reported in this paper.

### Data availability

Data will be made available on request.

### Acknowledgments

Many thanks to Prof. Antonio Leonardi and his Staff of the Hematology Department of AOU Federico II of Naples for making the irradiator available for measurements.

### References

- Anton, M., Büermann, L., 2015. Relative response of the alanine dosimeter to medium energy x-rays. *Phys. Med. Biol.* 60, 6113–6129.
- Araki, F., Ohno, T., Umeno, S., 2018. Ionization chamber dosimetry based on <sup>60</sup>Co absorbed dose to water calibration for diagnostic kilovoltage x-ray beams. *Phys. Med. Biol.* 63 (14pp), 185018.
- Ashland Advanced Materials Company, 2023. Retrieved from. <http://www.gafchromic.com/gafchromic-film/radiotherapy-films/index.asp>.
- Association for the Advancement of Blood & Biotherapies (n.d). Retrieved from AABB Blood Irradiation Guidelines: [www.aabb.org](http://www.aabb.org).
- Bakri, A., Mehta, K., Lance, D., 2021. Sterilizing insects with ionizing radiation. In: Dyck, J.H.V.A. (Ed.), *Sterile Insect Technique. Principles and Practice in Area-wide Integrated Pest Management*, second ed., pp. 355–398 (Chapter 3).4.
- Bartolotta, A., Onori, S., Pantaloni, M., 1989. Intercalibrazione dei metodi dosimetrici utilizzati presso gli impianti di irraggiamento industriale in Italia. *Ann. Ist. Super. Sanita* 25 (N. 2), 319–326.
- Bashir, S., Naik, F., Cardigan, R., Thomas, S., 2011. Effect of X-irradiation on the quality of red cell concentrates. *International Society of Blood Transfusion, Vox Sanguinis* 101, 200–207.

- Best Theratronics Ltd, 2011. Technical Specifications v.4.2011. Retrieved from. [www.theratronics.ca](http://www.theratronics.ca).
- Butler, D.J., Lye, J.E., Wright, T.E., Crossley, D., Sharpe, P.H., Stevenson, A.W., Crosbie, J.C., 2016. Absorbed dose determination in kilovoltage X-ray synchrotron. *Australas. Phys. Eng. Sci. Med.* 39, 943–950.
- Casolaro, P., Campajola, L., Breglio, G., Buontempo, S., 2019. Real-time dosimetry with radiochromic films. *Sci. Rep.* 1–11.
- Cleland, M.R., Stichelbaut, F., 2013. Radiation processing with high-energy X-rays. *Radiat. Phys. Chem.* 84, 91–99.
- D'Avino, V., Ambrosino, F., Bedogni, R., Campoy, A.I.C., La Verde, G., Vernetto, S., Vigorito, C.F., Pugliese, M., 2022. Characterization of thermoluminescent dosimeters for neutron dosimetry at high altitudes. *Sensors* 22 (15), 5721.
- Del Sol Fernández, S., García-Salcedo, R., Sánchez-Guzmán, D., Ramírez-Rodríguez, G., Gaona, E., de León-Alfaro, M.A., Rivera-Montalvo, T., 2016. Thermoluminescent dosimeters for low dose X-ray measurements. *Appl. Radiat. Isot.* 107, 340–345.
- Dodd, B., Vetter, R.J., 2009. Replacement of <sup>137</sup>Cs irradiators with X-ray irradiators. *Health Phys.* 96 – Issue 2, S27–S30.
- FDA-Food & Drug Administration. (n.d.). Retrieved from Recommendations regarding license amendments and procedures for Gamma Irradiation Of Blood Products: [www.fda.gov](http://www.fda.gov).
- Frentzel, K., Badakhshi, H., 2016. Irradiation with x-rays of the energy 18 MV induces radioactivity in transfusion blood: proposal of a safe method using 6 MV. *Med. Phys.* 43, 12.
- Horowitz, Y., 1984. *Thermoluminescence and Thermoluminescent Dosimetry*. CRC Press, Inc, Boca Raton, Florida.
- Hsi, W.C., Fagundes, M., Zeidan, O., Hug, E., Schreuder, N., 2013. Image-guided method for TLD-based in vivo rectal dose verification with endorectal balloon in proton therapy for prostate cancer. *Med. Phys.* 40, 5.
- Jacobs, G.P., 1998. A review on the effects of ionizing radiation on blood and blood components. *Radiat. Phys. Chem.* 53, 511–523.
- Knoll, G., 1999. *Radiation Detection and Measurement*. John Wiley Sons, Inc, New York.
- Liuzzi, R., Piccolo, C., D'Avino, V., Clemente, S., Oliviero, C., Cella, L., Pugliese, M., 2020. Dose response of TLD-100 in the dose range useful for hypofractionated radiotherapy. *Dose Response: Int. J.* 1–8.
- Liuzzi, R., Savino, F., D'Avino, V., Pugliese, M., Cella, L., 2015. Evaluation of LiF:Mg,Ti (TLD-100) for intraoperative electron radiation therapy quality assurance. *PLoS One* 1–11.
- Ma, C.-M., Chair Coffey, C.W., DeWerd, L.A., Liu, C., Nath, R., Seuntjens, J.P., 2001. AAPM protocol for 40–300 kV x-ray beam dosimetry in radiotherapy and radiobiology. *Med. Phys.* 28 (6), 868–893.
- Model 3500 Manual TLD Reader, 1993. Harshaw Bicon Radiation Measurement Products.
- Nasreddine, A., Kuntza, F., El Bitar, Z., 2021. Absorbed dose to water determination for kilo-voltage X-rays using alanine/EPR dosimetry systems. *Radiat. Phys. Chem.* 180.
- Nikolovski, S., Nikilovska, L., Velevska, M., Velev, V., 2010. Thermoluminescent signal fading of encapsulated LiF:Mg,Ti detectors in PTFE-Teflon. In: *Proceedings of the Second Conference on Medical Physics and Biomedical Engineering*.
- Nunn, A.A., Davis, S.D., Micka, J.A., DeWerd, L.A., 2008. LiF:Mg,Ti TLD response as a function of photon energy for moderately filtered x-ray spectra in the range of 20–250 kVp relative to <sup>60</sup>Co. *Med. Phys.* 35 (5), 1859–1869.
- Reuven, C., Pagonis, V., 2019. *Advances in Physics and Applications of Optically and Thermally Luminescence*. World Scientific Publishing Europe Ltd.
- Rudén, B., 1976. Evaluation of the clinical use of TLD. *Acta Radiol. Ther. Phys. Biol.* 15 (5), 447–464.
- Sharpe, P., Rajendran, K., Sephton, J.P., 1996. Progress towards an alanine/ESR therapy level reference dosimetry service at NPL. *Appl. Radiat. Isot.* 47 (No. 11/12), 117t–1175t.
- Simuta, Y.G., Parker, A., Cáceres, C., Vreysen, M.J., Yamada, H., 2021. Characterization and dose-mapping of an X-ray blood irradiator to assess application potential for the sterile insect technique (SIT). *Appl. Radiat. Isot.* 176, 109859.
- Soares, G.d., Squir, P.L., Pinto, F.C., Meira Belo, L.C., Grossi, P.A., 2009. Blood compounds irradiation process: assessment of absorbed dose using Ericke and Thermoluminescent dosimetric systems. In: *International Nuclear Atlantic Conference. ASSOCIAÇÃO BRASILEIRA DE ENERGIA NUCLEAR - ABEN, Rio de Janeiro, RJ, Brazil*.
- Soliman, Y.S., Pelliccioli, P., Beshir, W., Abdel-Fattah, A.A., Fahim, R.A., Krisch, M., Brüner-Krisch, E., 2020. A comparative dosimetry study of an alanine dosimeter with a PTW PinPoint chamber at ultra-high dose rates of synchrotron radiation. *Phys. Med.* 71, 161–167.
- Tachibana, H., Takahashi, R., Kogure, T., Nishiyama, S., Kurosawa, T., 2022. Practical dosimetry procedure of air kerma for kilovoltage X ray imaging in radiation oncology using a 0.6 cc cylindrical ionization chamber with a cobalt absorbed dose to water calibration coefficient. *Radiol. Phys. Technol.* 15, 264–270.
- Tadokoro, K., Reesink, H.W., Panzer, S., Chabanel, A., Santailier, G., Guérin, T., Snyder, E.L., 2010. Problems with irradiators. In: *International Society of Blood Transfusion, Vox Sanguinis*, vol. 98, pp. 78–84.
- Treleaven, J., Gennery, A., Marsh, J., Norfolk, D., Page, L., Parker, A., Webb, D., 2010. Guidelines on the use of irradiated blood components prepared by the British Committee for Standards in Haematology blood transfusion task force. *Br. J. Haematol.* 152, 35–51.

US National Academy of Science, 2008. Radiation Source Use and Replacement Study. [www.nationalacademies.org](http://www.nationalacademies.org).  
Waldeland, E., Malinen, E., 2011. Review of the dose-to-water energy dependence of alanine and lithium formate EPR dosimeters and LiF TL-dosimeters - comparison with Monte Carlo. *Radiat. Meas.* 46, 945–951.

Waldeland, E., Hole, E.O., Sagstuen, E., Malinen, E., 2010. The energy dependence of lithium formate and alanine EPR dosimeters for medium energy x rays. *Med. Phys.* 37 (7), 3569–3575.